with $B(E2, 2\rightarrow 4)$ values for similar nuclei obtained from lifetime measurements (and the rigid-rotor prediction). Since these $B(E2)$ values seem to be correct to within a few percent, we would expect that, from a $1/\eta$ variation, quantal corrections for ^{16}O excitation of the 4+ state are no larger than 1 or 2%. Of course, quantal corrections for excitation of the 6+ and 8+ states should be larger. However, our method of interpretation, which examines a ratio such as $P(6+)/P(4+)$, should eliminate a common portion of the quantal correction. In conclusion, we suspect it is unlikely that the observed departures of $B(E2)$ values from the rigid-rotor values are attributable to quantal corrections to the Coulomb-excitation process. There is, however, a distinct need for theoretical studies of quantal corrections to multiple Coulomb excitation.

To what extent can the present results on $B(E2)$ values be compared to other similar results? We have already mentioned that, to within the experimental errors, the $B(E2, 2\rightarrow 4)$ values for the good rotors agree with the rigid-rotor prediction. Lifetime measurements of similar 4+ states have produced $B(E2, 2\rightarrow 4)$ values of comparable accuracy and have also been in agreement with the rigid-rotor value.

The recent results from Berkeley on lifetimes measured by the "plunger" method make a particularly useful comparison with the present results. Diamond *et al.*[23] found the following values for ^{152}Sm:

$$B(E2, 2\rightarrow 4) = (1.87\pm 0.05)\times 10^{-48}\ e^2\ \mathrm{cm}^4$$

and

$$B(E2, 4\rightarrow 6) = (1.75\pm 0.09)\times 10^{-48}\ e^2\ \mathrm{cm}^4.$$

These values compare very well with our values of

$$B(E2, 2\rightarrow 4) = (1.94\pm 0.12)\times 10^{-48}\ e^2\ \mathrm{cm}^4$$

and

$$B(E2, 4\rightarrow 6) = (1.66\pm 0.17)\times 10^{-48}\ e^2\ \mathrm{cm}^4.$$

Diamond *et al.*[24] have also used the plunger method to measure the lifetimes of collective transitions in the nuclei $^{156,158,160}Er$. These nuclei are not very good rotors; the best is ^{160}Er, which has an $E(4+)/E(2+)$ ratio of 3.1. It is quite interesting that the $B(E2)$ values obtained for this rather poor rotor show no increase over the rigid-rotor values as one moves up the spin sequence. In fact, the $B(E2)$ values are smaller than the rigid-rotor values with assigned errors that barely overlap the rigid-rotor values. These lifetime results for ^{160}Er suggest the same trend in $B(E2)$ behavior as those we have established from multiple Coulomb excitation for the four good-rotor nuclei.

[23] R. M. Diamond, F. S. Stephens, R. Nordhagen, and K. Nakai, Proceedings of the of the International Conference on Properties of Nuclear States, Montreal, 1969 (unpublished), paper No. 2.7.

[24] R. M. Diamond, F. S. Stephens, W. H. Kelly, and D. Ward, Phys. Rev. Letters **22**, 546 (1969).

PHYSICAL REVIEW C VOLUME 1, NUMBER 4 APRIL 1970

Analysis of the ^{208}Pb(d, p)^{209}Pb g.s. Reaction

K. KING AND BRUCE H. J. MCKELLAR
Department of Theoretical Physics, University of Sydney, Sydney, New South Wales, Australia
(Received 16 October 1969)

The $^{208}Pb(d, p)^{209}Pb$ ground-state reaction is analyzed using the method of Butler, Hewitt, McKellar, and May. Using proton parameters fitted to elastic scattering data and Rosen's neutron parameters, good agreement with the proton angular distribution is obtained when the energy of the incident deuteron is above the Coulomb barrier. The spectroscopic factor extracted from the data is 0.65 ± 0.1.

I. INTRODUCTION

As an alternative to the distorted-wave Born-approximation (DWBA) approach to the theory of stripping reactions, Butler, Hewitt, McKellar, and May (BHMM)[1] proposed a method in which the cross section for the reaction (assuming spinless deuterons, neutrons, and protons) is written as

$$d\sigma/d\Omega = [S/(1-S)^2]\ |\ M_S\ |^2, \qquad (1)$$

where S is the spectroscopic factor. The matrix element M_S can be calculated from the optical potentials for the neutron and proton. The optical potential for the deuteron is not required. For generalization of Eq. (1) to the real world, in which particles have spins, we refer the reader to BHMM.

In the present paper, we discuss the application of Eq. (1) to the deuteron-stripping reaction on ^{208}Pb, which leads to the $2g_{9/2}$ ground state of ^{209}Pb. Experimental angular distributions for this reaction are available at several energies both above and below the Coulomb barrier, thus providing a useful test of the BHMM theory.

The neutron optical potential was not determined directly by optical-model analysis because there is a lack of sufficient neutron elastic-scattering data for the isotope ^{208}Pb. Our results show, however, that stripping calculations based on a combination of Rosen's neutron potential[2] and a proton potential that fits (p, p)

[1] S. T. Butler, R. G. L. Hewitt, B. H. J. McKellar, and R. M. May, Ann. Phys. (N.Y.) **43**, 282 (1967).

[2] L. Rosen, J. G. Beery, A. S. Goldhaber, and E. H. Auerbach, Ann. Phys. (N.Y.) **34**, 96 (1965).

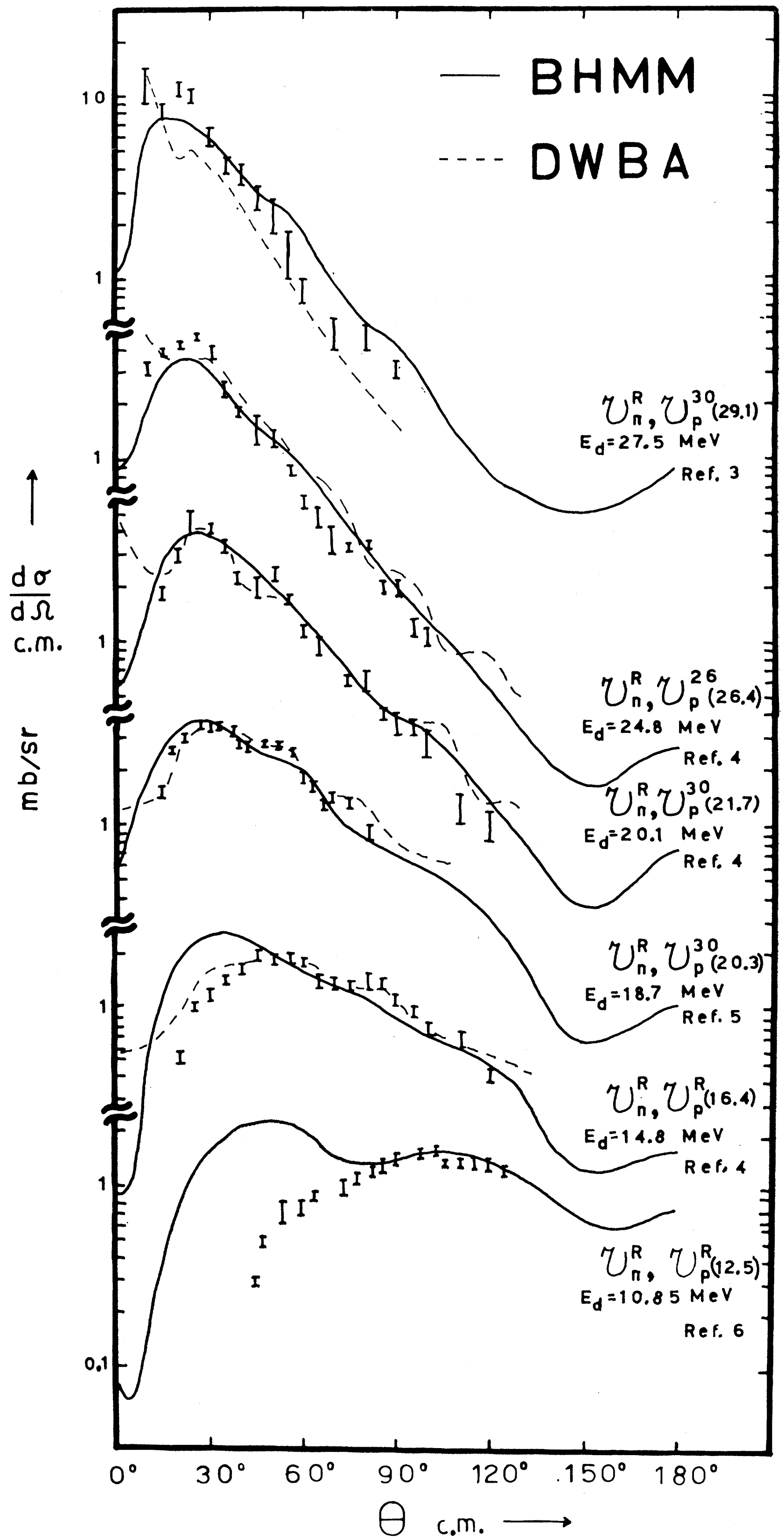

FIG. 1. Theoretical and experimental differential cross sections for the ^{208}Pb$(d,p)^{209}$Pb g.s. reaction at various bombarding energies. BHMM theoretical curves were generated using the optical-parameter sets indicated in code. See Tables II and III. Both the experimental data and the results of the DWBA calculations are contained in the references indicated.

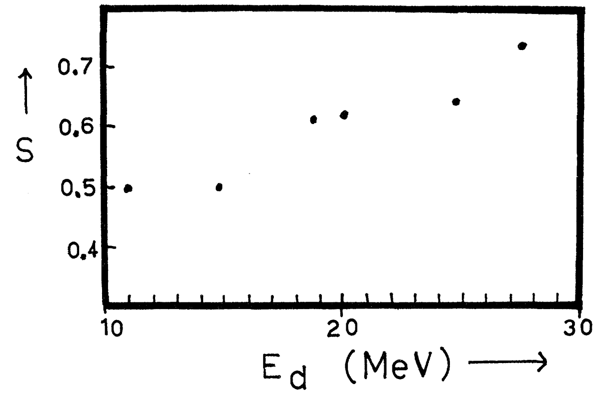

FIG. 2. Dependence of the spectroscopic factor on energy.

scattering data are in good agreement with experiment, provided the energy of the incident deuteron is above the Coulomb barrier (15.9 MeV). Below the barrier, the agreement is only qualitative. Because of the sudden approximation used for the deuteron wave function in BHMM, it is no surprise that the fit is better at higher energies. Typical results are shown in Fig. 1.

We also find that the average proton potential of Rosen[2] provides a fair basis for calculating the stripping cross sections in the 15–30-MeV energy range. While the calculated proton angular distributions were greatly improved by using proton potentials tailored to the ^{208}Pb(p, p)^{208}Pb data, spectroscopic factors extracted from the data did not change appreciably. This is similar to the result found by Butler, Hewitt, and Truelove[3] in their analysis of the ^{40}Ca(d, p)^{41}Ca ground-state reaction.

The values we obtain for the spectroscopic factors are given in Table I.[4–7] The extracted S values tend to increase with energy, but Fig. 2 shows that this does not occur in any systematic way. The variation of S with energy is no greater than that which occurs in the DWBA calculations. We therefore feel justified in suggesting a spectroscopic factor of 0.65 ± 0.1 for the ground state of ^{209}Pb. This is rather less than the shell-model value $S=1$, which one may have expected in the "doubly-magic–plus-one neutron" nucleus. Even very good shell-model nuclei can have $S<1$, however, because some of the single-particle strength leaks into neutron-continuum states[8] and because of hard-core correlations.[9]

In Sec. II, we discuss the choice of optical-model parameters and, in Sec. III, describe the results obtained in more detail.

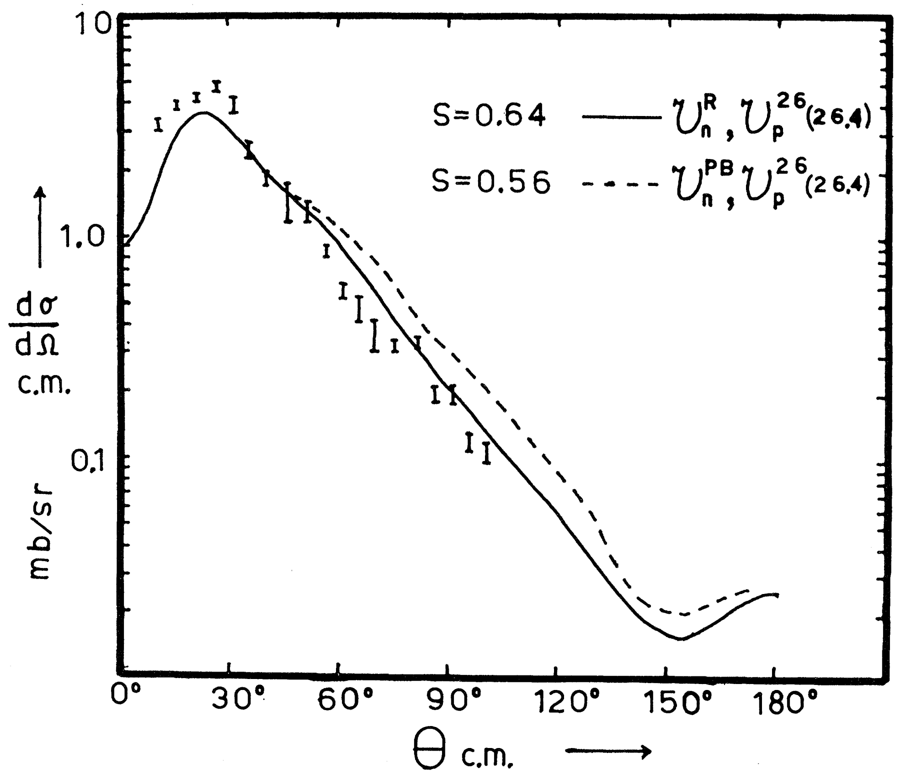

FIG. 3. Proton angular distributions for the ^{208}Pb(d, p)^{209}Pb g.s. reaction calculated with different standard neutron potentials but using the same proton potential. $E_d=24.8$ MeV.

---

[3] S. T. Butler, R. G. L. Hewitt, and J. S. Truelove, Phys. Rev. **162**, 1061 (1967).
[4] J. Testoni, S. Mayo, and P. E. Hodgson, Nucl. Phys. **50**, 479 (1964).
[5] G. Muehllehner, A. S. Poltorak, and W. C. Parkinson, Phys. Rev. **159**, 1039 (1967).
[6] A. F. Jeans, W. Darcey, W. G. Davies, K. N. Jones, and P. K. Smith, Nucl. Phys. **A128**, 224 (1969).
[7] M. T. McEllistrem, H. J. Martin, D. W. Miller, and M. B. Sampson, Phys. Rev. **111**, 1636 (1958).
[8] B. H. J. McKellar (to be published).
[9] B. H. Brandow, Rev. Mod. Phys. **39**, 771 (1967).

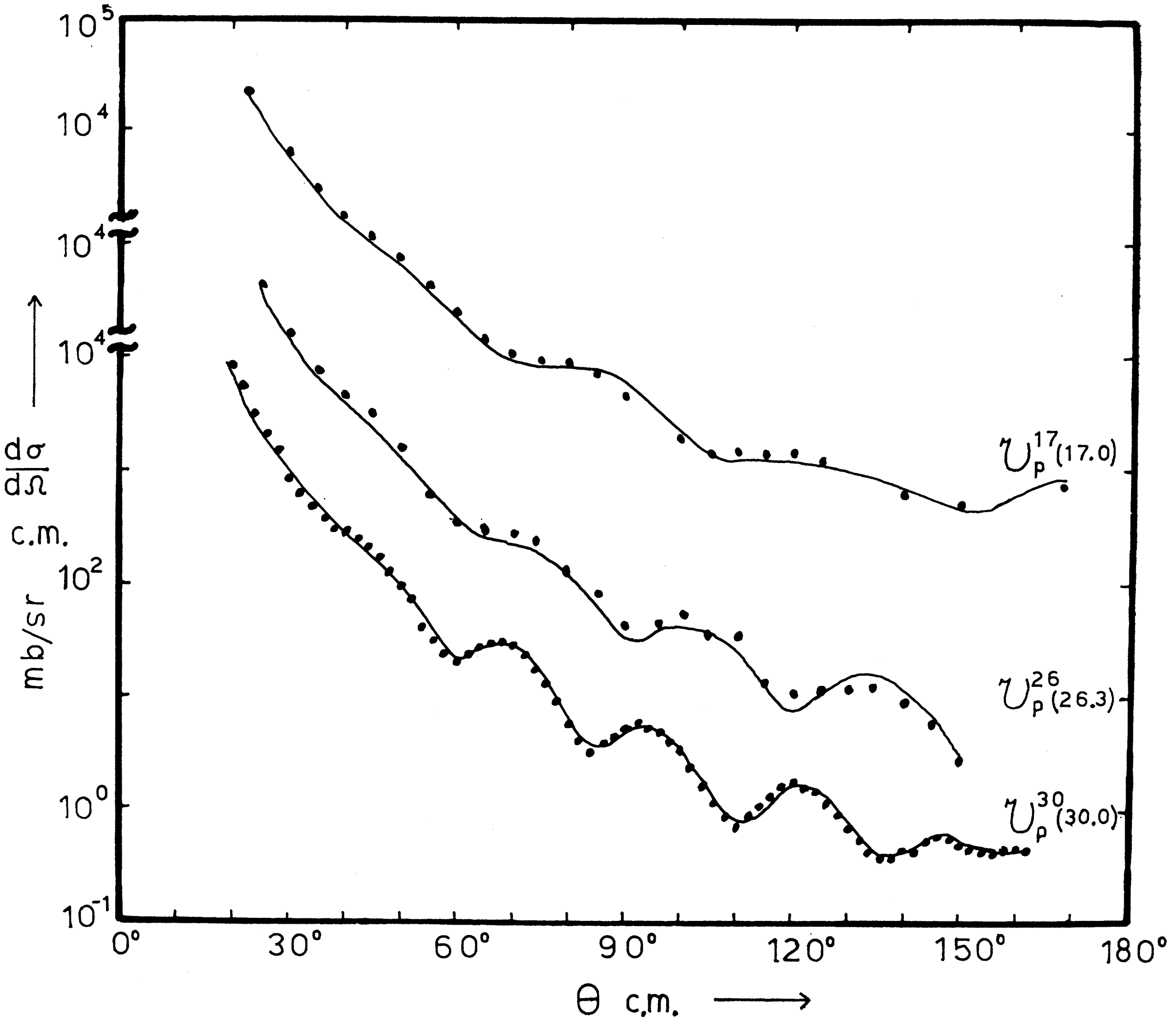

FIG. 4. Comparison of the experimental with the calculated proton elastic scattering cross sections. The proton optical potential used was found by fitting to these cross sections and to polarizations (shown in Fig. 5) where these were available.

II. OPTICAL-MODEL PARAMETERS

As pointed out above, the BHMM analysis makes no use of a deuteron optical potential. However, it does require proton and neutron optical potentials.

These nucleon-nucleus potentials we assume to have the form

$$V(r)=V_{\mathrm{Coul}}(r)-V_R f_R(r)-iW_V f_I(r)-iW_S g_I(r)-\lambda_\pi^2 V_{\mathrm{so}} h_{\mathrm{so}}(r)\mathbf{l}\cdot\boldsymbol{\sigma}. \quad (2)$$

Here V_{Coul} is the Coulomb potential of the nucleon in

TABLE I. Spectroscopic factors: Comparison of BHMM with DWBA.

Theory	Bombarding energy E_d (MeV) 10.85[a]	14.8[b]	18.7[c]	20.1[b]	24.8[b]	27.5[d]
BHMM	0.50	0.50	0.61	0.62	0.64	0.73
DWBA	···	0.87	0.82 ±0.16	0.77	0.67	0.9

[a] Reference 7; no DWBA fit to these data.
[b] Reference 5.
[c] Reference 6.
[d] Reference 4.

TABLE II. Optical parameters for neutron scattering.

Type	Code	Reference	V	W_V	W_S	V_{so}	r_R	r_I	r_{so}	a_R	a_I	a_{so}
Rosen	$\mathcal{V}_n^{R}$	a	$49.3-0.33E_n (E_n \leq 24$ MeV) $41.4-10.8 \ln(E_n/24) (E_n > 24$ MeV)	0.0	5.75	5.5	1.25	1.25	1.25	0.65	0.7	0.65
Perey-Buck (comparison set)	$\mathcal{V}_n^{PB}$	b	$48.0-0.29E_n (E_n \leq 24$ MeV) $41.0-10.8 \ln(E_n/24) (E_n > 24$ MeV)	0.0	9.6	7.2	1.27	1.27	1.27	0.66	0.47	0.66

[a] Reference 2.
[b] Reference 10.

TABLE III. Optical parameters for proton scattering.

Type	Code	References to parameters	References to scattering data	V	W_S	W_V	V_{so}	r_R	r_I	r_{so}	r_{Coul}	a_R	a_I	a_{so}
Rosen	$\mathcal{V}_p^{R}(E_p)$	a	a	$53.8-0.33E_p$	7.5	0.0	5.5	1.25	1.25	1.25	1.25	0.65	0.7	0.65
Buck	$\mathcal{V}_p^{B}(E_p)$	b	b	$52.6-0.28E_p$	10.6	0.0	8.0	1.25	1.25	1.25	1.25	0.65	0.47	0.65
Data fit	$\mathcal{V}_p^{17}(17.0)$	c	e	66.26	4.6	0.0	2.8	1.14	1.30	1.14	1.14	0.59	0.99	0.59
Data fit	$\mathcal{V}_p^{26}(26.3)$	d	d	48.89	2.9	10.2	3.2	1.25	1.25	1.25	1.25	0.65	0.47	0.65
Data fit	$\mathcal{V}_p^{30}(30.0)$	c	f	69.55	3.5	4.5	6.1	1.03	1.58	1.03	1.03	0.77	0.51	0.77

[a] Reference 2.
[b] Reference 12.
[c] These parameters found by the authors, using the SEEK code for optical-model analysis of elastic scattering data. See Ref. 11.
[d] Reference 14.
[e] Reference 13.
[f] References 14 and 15.

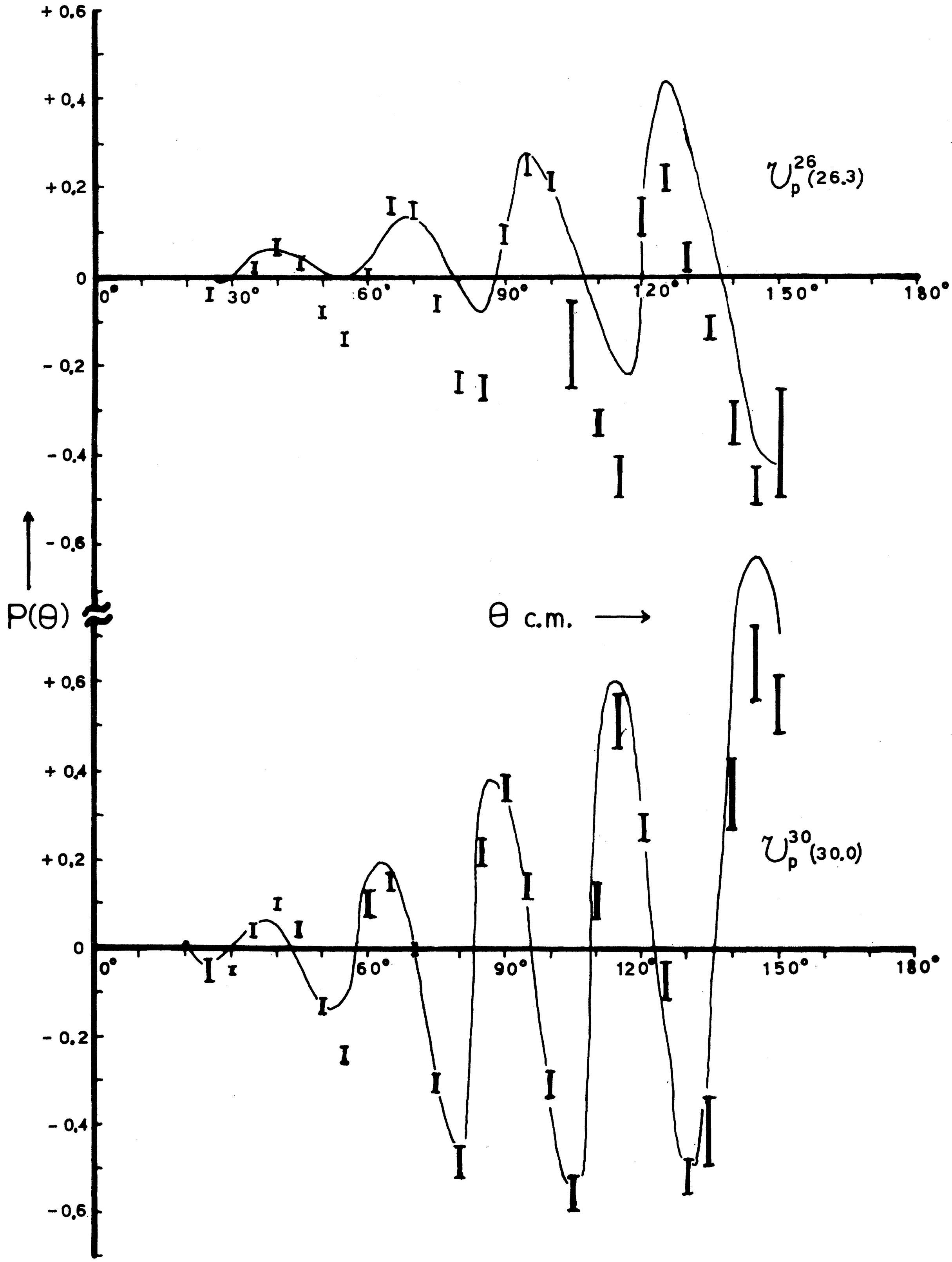

FIG. 5. Comparison of the experimental with the calculated proton polarizations resulting from elastic scattering on ^{208}Pb.

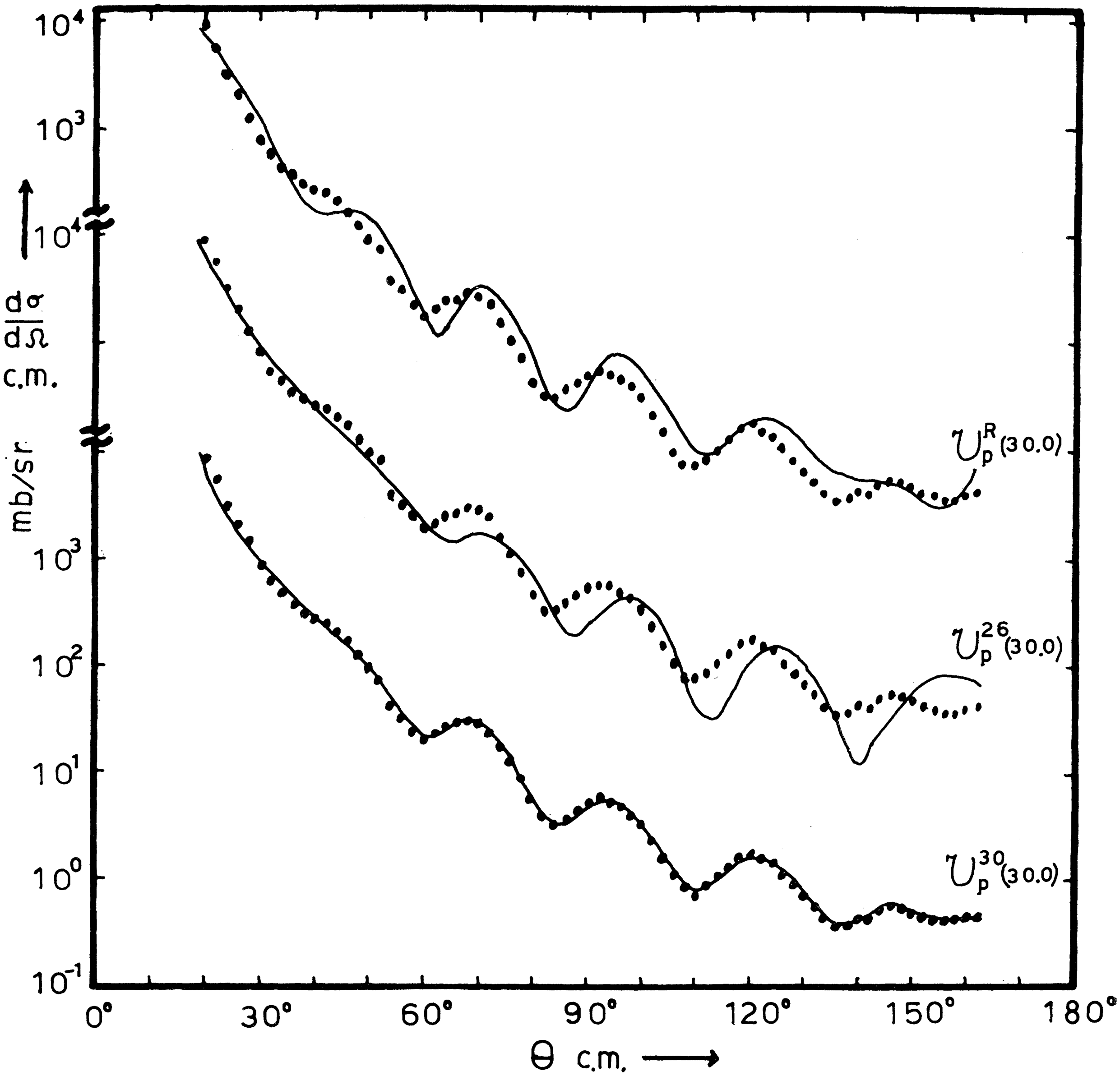

FIG. 6. The experimental cross sections for $^{208}Pb(p, p)^{208}Pb$ at a bombarding energy of 30 MeV compared to those calculated with various parameter sets. The good agreement is a demonstration of the validity of the extrapolation procedure. See also Figs. 7 and 8.

the field of a charge Ze distributed uniformly throughout the sphere $r \leq R$.

The depth of the real-potential well is V_R, the strength of the volume and surface absorptions are W_V and W_S, respectively, and the strength of the spin-orbit potential is V_{so}. All are measured in MeV. The dimensional factor $\lambda\!\!\!^{-}_\pi$ is the pion Compton wavelength, which is taken as exactly $\sqrt{2}$ F. The orbital angular momentum is $\hbar\mathbf{l}$.

The volume form factors $f(r)$ are taken to have the Woods-Saxon form, e.g.,

$$f_R(r) = \{1+\exp[(r-r_R A^{1/3})/a_R]\}^{-1} \tag{3}$$

with radius $r_R A^{1/3}$ and diffuseness a_R. The form factors $g_I(r)$ and $h_{so}(r)$ are given by

$$g_I(r) = -4a_I[df_I(r)/dr],$$
$$h_{so}(r) = (1/r)[df_{so}(r)/dr]. \tag{4}$$

The bound-state neutron potential[1] (which is wholly real) is of the form

$$V_{bs}(r) = -V_R' f_R(r) - \lambda\!\!\!^{-}_\pi{}^2 V_{so}' h_{so}(r) \mathbf{l}\cdot\boldsymbol{\sigma}. \tag{5}$$

The spin-orbit term is chosen to be 25 times the Thomas term, i.e.,

$$V_{so}' = 25(M_\pi^2/4M_p^2)V_R' = 0.138V_R',$$

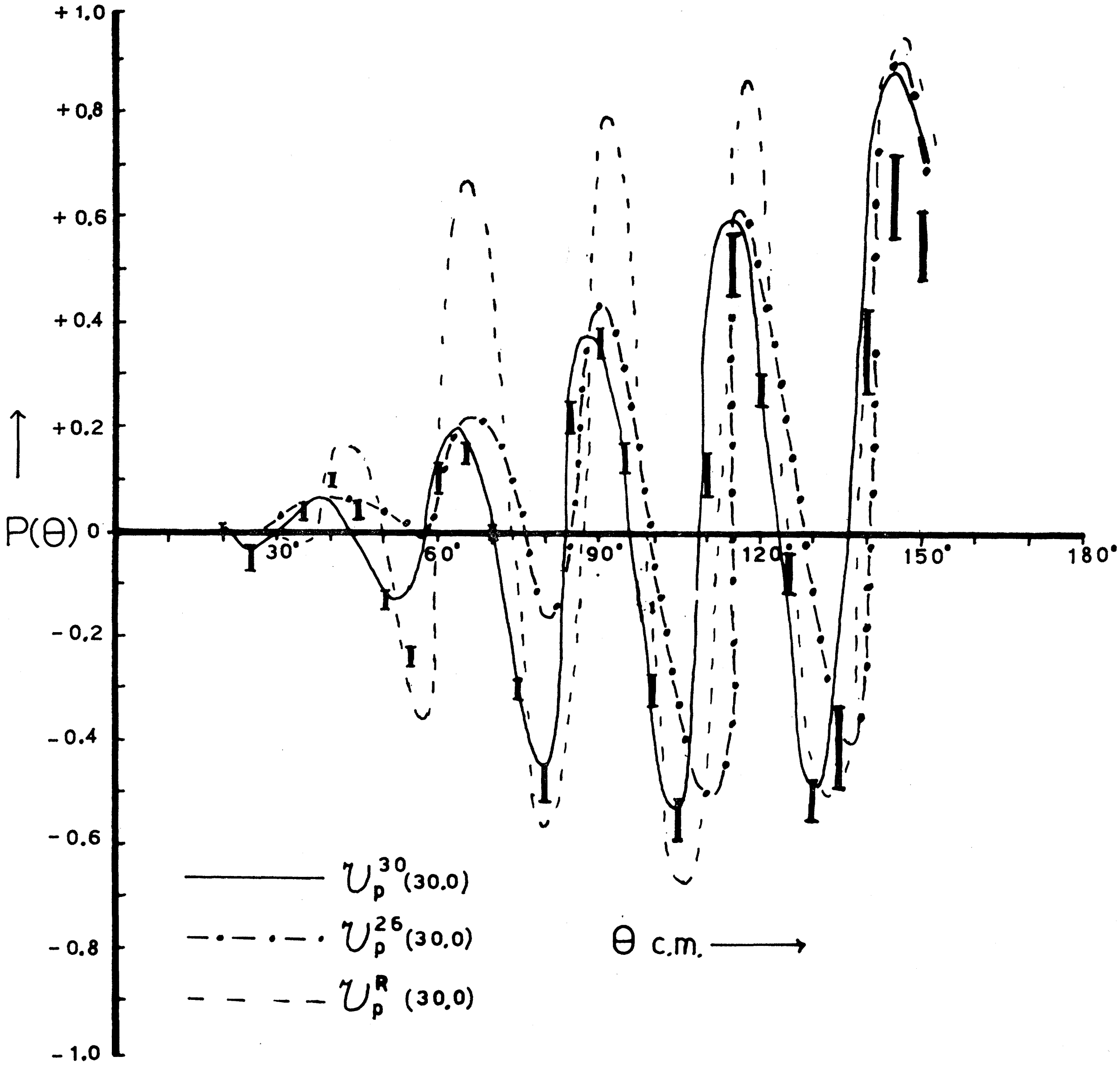

FIG. 7. The experimental proton polarizations from $^{208}Pb(p, p)^{208}Pb$ at a bombarding energy of 30 MeV compared to the predictions of various proton potentials.

where the strength of the central potential V_R' is chosen so as to provide the correct binding energy for the bound-state neutron. V_R' and V_{so}' so chosen are close to the values V_R and V_{so} for the scattered-neutron potential.

A. Neutron Potential

The BHMM analysis requires the neutron optical potential for a wide range of neutron energies—0 to 100 MeV for the cases considered. Unfortunately, there is very little data on the elastic scattering of neutrons on ^{208}Pb. We therefore selected the Rosen neutron potential[2] as our neutron optical potential. The parameters of this potential, which we refer to as $\mathcal{V}_n^R$ are listed in Table II, together with the parameters of the other standard neutron potential of Perey and Buck[10] (which we refer to as $\mathcal{V}_n^{PB}$).

Figure 3 shows the (d, p) angular distributions obtained using $\mathcal{V}_n^R$ and $\mathcal{V}_n^{PB}$ with the same proton potential at an incident deuteron energy of 24.8 MeV. Better agreement is displayed by calculations using $\mathcal{V}_n^R$, whereas the difference in the spectroscopic factors extracted by the two results is only slight. This behavior is characteristic at all energies.

[10] F. Perey and B. Buck, Nucl. Phys. **32**, 353 (1962).

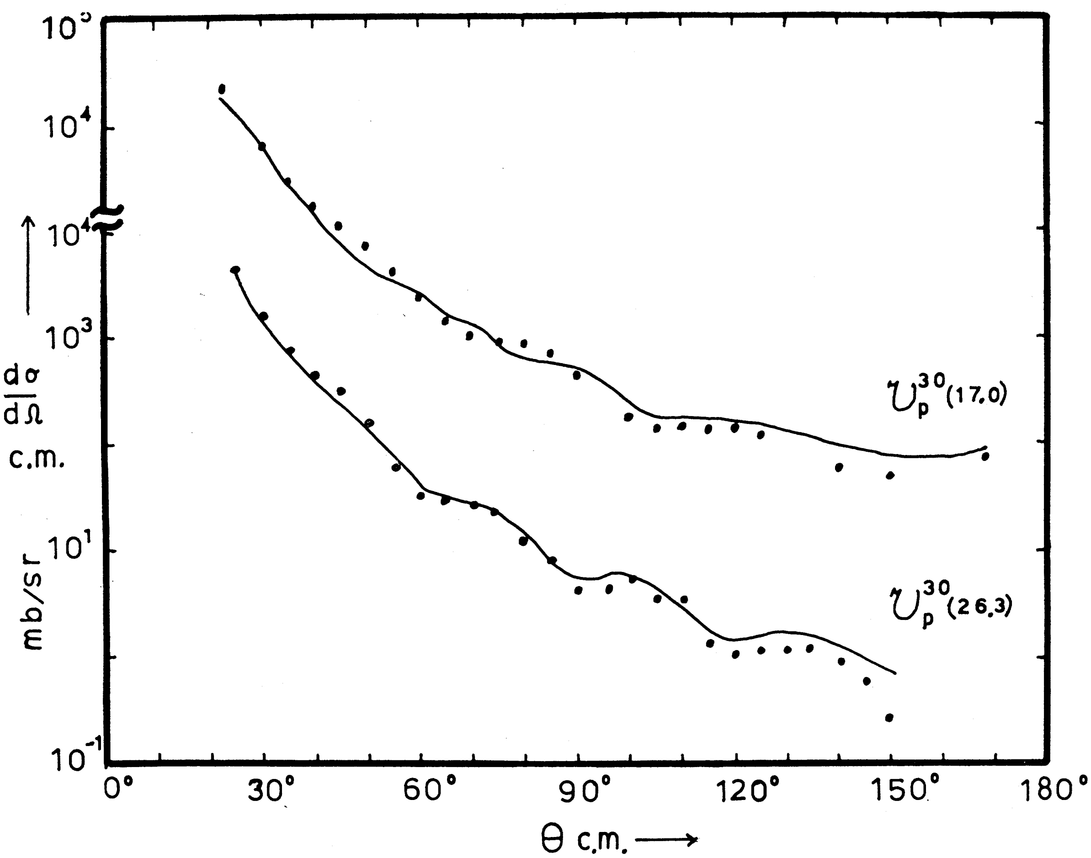

FIG. 8. The experimental cross sections for proton elastic scattering at 17.0 and 26.3 MeV compared to the predictions of potentials extrapolated from the one fitted to 30.0-MeV data.

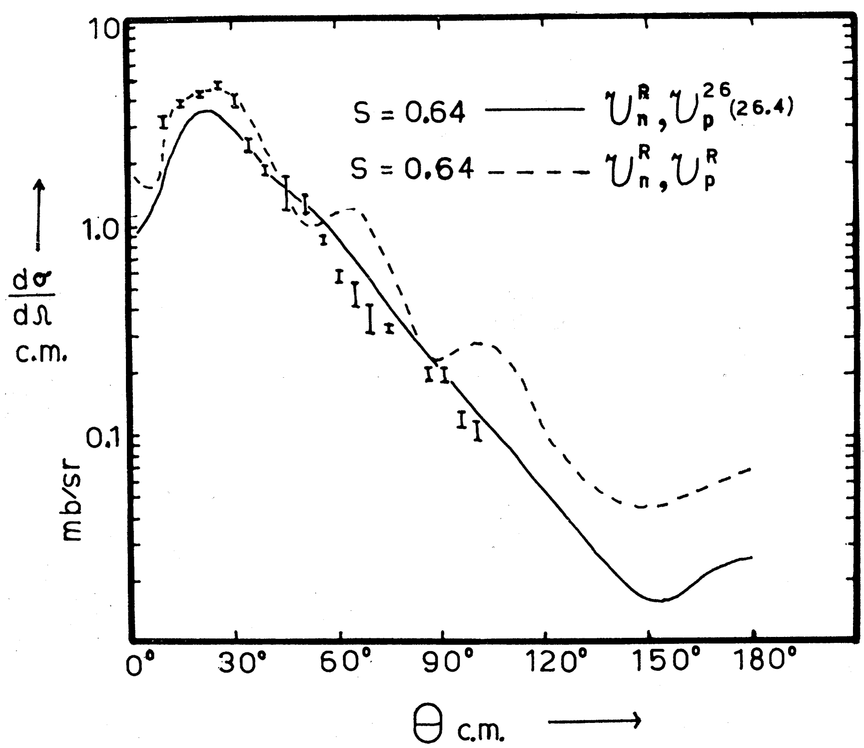

FIG. 9. Comparison of the proton angular distribution in the ^{208}Pb(d, p)^{209}Pb g.s. reaction calculated using Rosen's proton potential to that obtained using the proton potential fitted to the elastic scattering data. (The Rosen neutron potential was used in both cases.) $E_d = 24.8$ MeV.

B. Proton Potential

The proton optical potential is required only at the energy of the outgoing proton.

Proton elastic scattering data was available at energies near some of those at which we require the proton optical potential. At these energies E, we calculated a best-fit potential $\mathcal{V}_p{}^E$ using the SEEK code,[11] or we used a best-fit potential if this data were supplied. The parameters of these potentials are given in Table III,[12–15] together with those of the standard optical potentials of Rosen *et al.*[2] ($\mathcal{V}_p{}^{\mathrm{R}}$) and Buck[12] ($\mathcal{V}_p{}^{\mathrm{B}}$).

The potentials $\mathcal{V}_p{}^{\mathrm{R}}$ and $\mathcal{V}_p{}^{\mathrm{B}}$ have geometrical parameters and all well depths fixed except V_R. The real well depth V_R varies linearly with energy. We adopted the same linear variation of V_R with energy whenever we extrapolated $\mathcal{V}_p{}^E$ to another proton energy E', this extrapolated potential being referred to as $\mathcal{V}_p{}^E(E')$.

In Fig. 4, we show a comparison of the observed differential cross sections at energies 17.0, 26.3, and 30.0 MeV, with the cross sections predicted by the potentials $\mathcal{V}_p{}^{\mathrm{R}}(17.0)$, $\mathcal{V}_p{}^{26}(26.3)$, $\mathcal{V}_p{}^{30}(30.0)$, which we use to generate (d, p) cross sections. In Fig. 5, we show a similar comparison of polarization data.

To illustrate the validity of the extrapolation procedure, Figs. 6 and 7 compare the differential cross section and polarization observed at 30 MeV with those predicted by various extrapolated potentials. It will be seen that the theoretical differential cross sections always match the experimental ones well, although the agreement with polarization data is much more sensitive to the particular potential used.

In Fig. 8, we compare the calculated proton elastic scattering cross sections given by $\mathcal{V}_p{}^{30}$ to those measured at 17 and 26 MeV.

As the data at 30 MeV are the most extensive, we think that $\mathcal{V}_p{}^{30}$ is the best potential with which to extrapolate to energies where (p, p) data is unavailable.

TABLE IV. Spectroscopic factors (BHMM): Comparison of potentials used.

Potentials	Bombarding 18.7	Energy 20.1	24.8	E_d (MeV) 27.5
$\mathcal{V}_n{}^{\mathrm{R}}$ with proton parameters fitted to scattering data.	0.61	0.62	0.64	0.73
$\mathcal{V}_n{}^{\mathrm{R}}$ with $\mathcal{V}_p{}^{\mathrm{R}}$	0.61	0.61	0.64	0.77

[11] M. A. Melkanoff, T. Sawada, and J. Raynal (private communication).
[12] B. Buck, Phys. Rev. **130**, 712 (1963).
[13] G. Schrank and R. E. Pollock, Phys. Rev. **132**, 2200 (1963).
[14] D. L. Watson, J. Lowe, J. C. Dore, R. M. Craig, and D. J. Baugh, Nucl. Phys. **A92**, 193 (1967).
[15] B. W. Ridley and J. F. Turner, Nucl. Phys. **58**, 497 (1964).

III. RESULTS AND CONCLUSION

Our major results are presented in Figs. 1 and 2. Using BHMM theory, we obtain good agreement between the calculated and measured proton angular distributions of the ^{208}Pb$(d, p)^{209}$Pb ground-state reaction at incident deuteron energies above the Coulomb barrier. The spectroscopic factor so extracted is 0.65 ± 0.1.

We think that a spectroscopic factor rather less than unity should be taken seriously even for such a good shell-model nucleus as ^{209}Pb. Even discounting the possibility of mixing with vibrational states of the core, there are two sources of depletion of the single-particle strength. It is well known that hard-core correlations in nuclei shift some of the strength to very high excitations. Brandow[9] quotes the estimate that S is reduced by 15–20% in this way. McKellar[8] has estimated that coupling to continuum neutron channels introduces a further depletion of the order of $\mathrm{Im}\mathcal{V}_n/\mathrm{Re}\mathcal{V}_n$, which is about 10% for the Rosen potential. A spectroscopic factor of 0.65 for ^{209}Pb is consistent with these estimates.

Note added in proof. We have recently been reminded of a calculation of the depletion of the single-particle strength in ^{209}Pb by coupling to vibrational states of the core [G. F. Bertsch and T. T. S. Kuo, Nucl. Phys. **A112**, 204 (1968)]. A depletion of 15 to 25% is found, providing further evidence that small spectroscopic factors are reasonable.

Another important feature of the analysis is the observation that, while the angular distribution is sensitive to the proton potential, the spectroscopic factor is not. In Fig. 9, we compare the differential cross section for incident deuterons at 24.8 MeV with curves calculated using the average proton potential $\mathcal{V}_p{}^{\mathrm{R}}(26.4)$ and a potential $\mathcal{V}_p{}^{26}(26.4)$ fitted to (p, p) data.[14] Table IV compares spectroscopic factors obtained using Rosen potentials with those derived from best-fit potentials. We conclude that reliable spectroscopic factors may be extracted using average potentials.

ACKNOWLEDGMENTS

It is a pleasure to thank Professor S. T. Butler for helpful discussions. The authors are also indebted to Dr. R. G. L. Hewitt and J. S. Truelove, who provided them with the BHMM code. This work was supported in part by the Science Foundation for Physics within the University of Sydney, and we are grateful to its Director, Professor H. Messel, for his support.